AN EXPERIMENTAL STUDY OF A SELF-ACTING FOIL BEARING AT LOW VALUES OF FOIL TENSIONS

by

John Michael Knight

DUDLEY KNOX LIBRARY
NAVAL POSTGRADUATE SCHOOL
MONTEREY CA 93943-5101

Gaylord
SHELF BINDER
Syracuse, N. Y.
Stockton, Calif.

UNITED STATES
NAVAL POSTGRADUATE SCHOOL

THESIS

AN EXPERIMENTAL STUDY OF A SELF-ACTING FOIL BEARING AT LOW VALUES OF FOIL TENSION

by

John Michael Knight

September 1968

This document is subject to special export [redacted]

DOWNGRADED
APPROVED FOR PUBLIC RELEASE

LIBRARY
NAVAL POSTGRADUATE SCHOOL
MONTEREY, CALIF. 93940

AN EXPERIMENTAL STUDY OF A SELF-ACTING FOIL BEARING AT LOW VALUES OF FOIL TENSION

by

John Michael Knight
Lieutenant, United States Navy
B.S., University of California at Berkeley, 1963

Submitted in partial fulfillment of the
requirements for the degree of

MASTER OF SCIENCE IN MECHANICAL ENGINEERING

from the

NAVAL POSTGRADUATE SCHOOL
September 1968

THESIS
K62
c.1

ABSTRACT

Theoretical solutions for the gap thickness in an infinitely wide foil bearing are reviewed. An experiment is described using a stainless steel foil wrapped about a high speed rotor. Details of instrumentation are included. Results are presented for the relation between gap thickness and foil stiffness for low values of foil tension.

Only a small amount of data was obtained due to failure of the rotor support mechanism. The results are therefore inconclusive. The results do, however, indicate a dependence of foil gap thickness on foil stiffness. The influence of fluid inertia on foil gap thickness is also indicated although this effect appears to be small compared to the effects of foil stiffness.

LIBRARY
NAVAL POSTGRADUATE SCHOOL
MONTEREY, CALIF. 93940

TABLE OF CONTENTS

Section		Page No.
1.	Introduction	11
2.	Review of Literature	13
3.	Theoretical Considerations	17
4.	Experimental Procedure	25
5.	Instrumentation	28
6.	Results	30
7.	Discussion of Results	31
8.	Recommendations	34
	Bibliography	36
	Tables	38
	Figures	42
	Appendix A: Distance Probe Calibration .	58

LIST OF FIGURES

Number	Title	Page No.
1.	Typical Foil Bearing Configuration	42
2.	Nominal Clearance vs Stiffness and Compressibility Parameters	43
3.	Nominal Clearance vs Inertia Parameter . .	44
4.	Cut-away View of Test Assembly	45
5.	Test Assembly, Side View (Photograph) . .	46
6.	Test Assembly, Top View (Photograph) . . .	47
7.	Rotor (Photograph)	48
8.	Instrumentation Layout	49
9.	Instrumentation (Photograph)	50
10.	Gap Thickness vs Velocity	51
11.	Gap Thickness vs Foil Bearing Number . . .	52
12.	Nominal Clearance vs Stiffness Parameter .	53
13.	Nominal Clearance vs Inertia Parameter . .	54
14.	Calibration Curve	55
15.	Comparator (Photograph)	56
16.	Foil Gap Calibration Curve	57

LIST OF SYMBOLS

Symbol	Description
C	Compressibility Parameter = $P_o r_o/T$
D	Flexural Rigidity of Foil Per Unit Width
E	Modulus of Elasticity
h	Radial Clearance or Gap Thickness
h^*	Nominal Clearance (where $dP/d\theta = 0$)
H	Dimensionless Clearance = $(h/r_o)\epsilon^{-2/3}$
H^*	Dimensionless Nominal Clearance = $(h^*/r_o)\epsilon^{-2/3}$
I	Inertia Parameter = $\frac{1}{2}\rho U^2/T/r_o$
k,m,n	Exponential Measures
M	Bending Moment Per Unit Width
P	Pressure Under Foil
P_o	Ambient Pressure
Q	Shear Force Per Unit Width
r	Radial Position
r_o	Rotor Radius
R	Local Radius of Curvature
s	Distance Along Foil = $r\theta$
S	Stiffness Parameter = $(D\epsilon^{-2/3})/T_\infty r_o^2$
T	Tension Per Unit Width
T_∞	Tension Per Unit Width at ∞
t	Thickness of Foil
U	Relative Speed Between Rotor and Foil
$\hat{u}$	Dimensionless Angular Velocity Component
V	Velocity Component in Radial Direction
$\hat{v}$	Dimensionless Radial Velocity Component

X	Non-dimensional Clearance = h/r_o
X^*	Nominal Non-dimensional Clearance = h^*/r_o
ϵ	Foil Bearing Number = $6\mu U/T$
μ	Air Viscosity
ρ	Air Density
γ	Poisson Ratio
π	Dimensionless Pressure
θ	Polar Angle
ξ	Extended Coordinate = $\theta \epsilon^{-1/3}$
η	Dimensionless Distance from Rotor
σ	Internal Stress in Foil

ACKNOWLEDGEMENTS

Several people have been extremely helpful to me during this project.

Mr. Manfred Wildman of the Ampex Corporation was very generous in providing assistance when the rotor and bearings required remachining. Without his help, no data could have been obtained.

Dr. Abe Eshel, also of the Ampex Corporation, has been extremely helpful in leading me to some small understanding of the extensive theoretical work he has done in the foil bearing field.

Professor Paul Pucci has been very generous with his time in rendering both advice and encouragement.

My wife Diane has been very helpful and has found time to type this manuscript.

1. Introduction

The subject of this study is a foil type bearing. Such a bearing consists of a compliant film moving relative to a rigid cylinder. Figure 1 illustrates a typical foil bearing schematically. This bearing configuration has found application in the high speed tape transport systems of digital computers, in the manufacture of cloth and in fact, anywhere that a film moves over a surface with high relative speed.

Of particular interest in a study of the foil bearing is the thickness of the lubricating film; that is, the gap thickness between the foil and the cylinder. Also of interest is the contour of the foil around the cylinder. Intuitively we expect that the gap thickness will be affected by physical conditions characterized by the following physical quantities: relative speed between foil and cylinder; foil tension and foil stiffness; and lubricant density, viscosity, and compressibility.

Several non-dimensional parameters have been devised to indicate the relative importance of specific physical effects on the foil bearing. The foil bearing number relates the viscous forces in the lubricating film to the average pressure above atmospheric in the film. The compressibility parameter relates the ambient pressure to the average pressure above atmospheric in the film. The inertia parameter relates the fluid inertia forces to the average pressure above atmospheric in the film. The stiffness parameter relates the bending

moment in the foil to the moment of the foil tension about the cylinder axis.

A mathematically convenient idealization of the foil bearing problem can be obtained by making the following assumptions: the foil is infinitely wide; the foil is perfectly flexible; the lubricating gas is incompressible; inertia forces are negligible. These assumptions correspond to setting the inverse compressibility parameter, the stiffness parameter and the inertia parameter equal to zero. Several analyses have been made with these assumptions imposed. The results of these analyses have shown that the nominal gap width is equal to a constant times the foil bearing number to the 2/3 power. These results are valid for a broad range of foil bearing applications.

The purpose of this experiment is to investigate the effects of stiffness on the gap width. A convenient way to include the effect of stiffness is to consider its effect on the results of the ideal solution. Since a theoretical study of this nature is available, it can be used for comparison with experimental results.

2. Review of Literature

A comprehensive review of the literature pertaining to the foil bearing is presented by L. Licht (10). Some of the articles he has reviewed are mentioned here along with some others that have been published recently.

The first study of the foil type bearing was an experiment by H. Blok and J. van Rossum (1). They also included an analytical discussion. They present a solution for the nominal gap width as a constant times the foil bearing number to the 2/3 power. This result is derived from the Reynolds equation. The assumption that the foil contour in the inlet region is parabolic is also used. Use of the Reynolds equation to describe the fluid behavior assumes negligible fluid inertia and fluid incompressibility.

Cameron and Patel (2) derived a less restrictive differential equation for the gap thickness than Blok and van Rossum. They employ the Reynolds equation in polar coordinates. The pressure term in this equation is eliminated by assuming negligible foil stiffness. In this case equilibrium requires the fluid pressure to be equal to the ratio of the foil tension to the local radius of curvature. Only first order terms in the equation for the radius of curvature in polar coordinates are retained. They did not present a solution to this equation.

Baumeister (3) presents a solution to the Cameron-Patel equation. This solution is obtained using numerical methods. He also presents solutions to more complicated differential

equations which are derived in the manner of the Cameron-Patel equation but retain second and higher order terms in the expression for the local radius of curvature. He does not indicate the details of the numerical analysis.

Eshel and Elrod (5) have presented a more refined and elaborate solution for the nominal gap width than those already mentioned. They employ the same limiting assumption as Cameron and Patel and Baumeister. In this work Eshel and Elrod utilize a small perturbation analysis to reduce the Reynolds equation to a zeroth order differential equation in a non-dimensional film thickness. Details of the numerical analysis are also presented. Extension of their solution into the exit region indicates the presence of undulations in the foil contour.

Eshel and Elrod (6) have studied the effects of foil stiffness on the gap width. In this analysis all the assumptions of their earlier analysis are imposed except that of negligible foil stiffness. The results of this analysis are presented as a correction curve to the results obtained in their more restrictive paper (5).

In a further refinement of their basic study, Eshel and Elrod (7) have studied the effects of compressibility on the nominal gap width. Again all of the original limiting assumptions are made except that of fluid incompressibility. As in their study of stiffness effects, the results are presented as a correction curve to the results presented in the first paper (5).

Several experimental studies have been conducted by L. Licht (8), (9), and (10). Licht uses a small capacitive probe mounted in the rotor to measure the gap thickness directly. Experiments are conducted with metalic foils as well as with more flexible Mylar foils coated with a conducting film. Results of these experiments corroborate the theoretical results of Baumeister, and Eshel and Elrod. Licht also presents oscillographs which show the undulations of the foil in the exit region.

Experiments made by Ma (11) also are in agreement with the theory of Eshel and Elrod and Baumeister. Ma employed a rectangular probe mounted on a rotating drum. The probe spanned three-fourths of the foil width and measured the average gap thickness directly.

Licht and Eshel (16) have recently presented a thorough study of a foil rotor support system. A high speed rotor is supported by three symetrically located foil segments, each of which has a 60 degree angle of wrap about the rotor. Foil gap, foil contour, and response of the system to various imposed disturbances are studied. Applicable theoretical considerations are presented in detail.

Eshel (17) has recently made an analytical study of the influence of fluid inertia forces on the nominal gap width. This study has necessitated a new reduction of the Navier-Stokes equations. In this analysis he has also included the effects of fluid compressibility. Eshel has reduced the Navier-Stokes equations to Prandtl's boundary

layer equations. These equations are solved simultaneously using numerical methods. The solution is presented in the form of correction curves to the results obtained in his basic study (5).

3. Theoretical Considerations

The governing equations for the fluid behavior in a foil bearing, as in many fluid problems, are the Navier-Stokes equations. Several physically reasonable assumptions pertaining to the foil bearing can be made that will reduce these complicated equations. These assumptions are listed here.

(1) The foil bearing is infinitely wide.

(2) The fluid flow is steady and one dimensional.

(3) The gap thickness is small compared to the cylinder radius.

(4) The fluid is incompressible.

(5) Inertia forces are small compared to viscous forces.

With these assumptions imposed the governing equation of lubrication for the foil bearing becomes the Reynolds equation.

$$d/ds(h^3 dP/ds) = \pm 6\mu U\ (dh/ds) \qquad [1]$$

h = the thickness of the gap between the foil and the cylinder

P = the fluid pressure

s = the distance along the cylinder

U = the relative velocity between the foil and the cylinder

μ = the fluid viscosity

Gross (12) presents a thorough derivation of this equation from the Navier-Stokes equations.

Blok and van Rossum (1) assumed that

$$h = h^* + s^2/2r_o \qquad [2]$$

where h^* = the nominal gap thickness (where $dP/ds = 0$).

They obtained the following equation for the nominal gap thickness.

$$h^*/r_o = .426(6\mu U/T)^{2/3} \qquad [3]$$

Cameron and Patel (2) expressed the Reynolds equation in polar coordinates.

$$d/d\theta(h^3\, dP/d\theta) = \pm\, 6\mu Ur(dh/d\theta) \qquad [4]$$

$h = r - r_o$

r = the radial coordinate

θ = the angular coordinate

They also introduced the non-dimensional coordinate

$$X = h/r_o .$$

They assumed a perfectly flexible foil so that equilibrium of the foil required that

$$P - P_o = T/R \qquad [5]$$

where R = the local radius of curvature

T = the foil tension per unit width

P_o = the ambient pressure

The radius of curvature in polar coordinates is

$$R = \frac{\left[(dr/d\theta)^2 + r^2\right]^{3/2}}{2(dr/d\theta)^2 - r(d^2r/d\theta^2) + r^2} \quad . \qquad [6]$$

Expanding this relationship for curvature, and retaining only terms of 1st order, and using equation [5] to eliminate the pressure term from the Reynolds equation, a non-dimensional differential equation is obtained.

$$d/d\theta(X + d^2X/d\theta^2) = \pm (6\mu U/T)(X - X^*)/X^3 \qquad [7]$$

X^*= the nominal non-dimensional gap thickness

Baumeister (3), (4) has solved this equation using numerical methods and has obtained the following equation.

$$h^*/r_o = .639\ (6\mu U/T)^{2/3} \qquad [8]$$

He also has solved a more complicated equation derived as above but retaining second and higher order terms in the expansion of the curvature equation. This result is as follows:

$$h^*/r_o = .650\ (6\mu U/T)^{2/3} \qquad [9]$$

Eshel and Elrod (5) have provided a more refined solution for the nominal gap width. The assumptions made are the same as those mentioned above. The derivation of the differential equation employs a similar approach to that of Cameron and Patel except the non-dimensional film thickness is assumed to be

$$h/r_o = H(\theta)\epsilon^n \qquad [10]$$

where $H(\theta)$ = the non-dimensional gap thickness

ϵ = a small parameter

n = an undetermined exponent

$$h^*/r_o = H^*\epsilon^n .$$

They also introduce an extended coordinate

$$\xi = \theta\epsilon^{-m} \qquad [11]$$

where m = an undetermined exponent.

In addition, a non-dimensional pressure is defined.

$$\pi = (P - P_o)r_o/T = Tr_o/TR = r_o/R \qquad [12]$$

Using these equations π can be expressed as a series in ϵ so that

$$\pi = 1 + (d^2H/d\xi^2)\epsilon^{n-2m} + (dH/d\xi)^2/2 + 2H(dH/d\xi)\epsilon^{2n-2m} - H\epsilon^n + 3/2(d^2H/d\xi^2)(dH/d\xi)^2\epsilon^{3n-2m} + \cdots\cdots \qquad [13]$$

Equation [4] can then be reduced to

$$d/d\xi(H^3 d\pi/d\xi)\epsilon^{3n-2n} = \mp (6\mu U/T)(dH/d\xi)\epsilon^{n-m} \qquad [14]$$

By applying the boundary conditions of the problem to equations [13] and [14], they show that

$n = 2/3$ $\qquad$ $m = 1/3$

$\epsilon = 6\mu U/T$, the foil bearing number which relates viscous forces to the average pressure above ambient in the fluid.

H is then expanded into a series in ϵ, where

$$H = H_o + H_1\epsilon^{2/3} + \cdots \qquad [15]$$

$$H^* = H_o^* + H_1^*\epsilon^{2/3} + \cdots .$$

Using equation [13] in equation [14] to eliminate π, a family of differential equations is obtained. The zeroth order equation is

$$d^3H_o/d\xi^3 = \mp (H_o - H_o^*)/H_o^3 . \qquad [16]$$

Since ϵ is a small parameter it is reasonable to accept the zeroth order approximation for H^*. Eshel and Elrod obtain $H^* = .643$ so that in the region of uniformity

$$h^*/r_o = .643\epsilon^{2/3} . \qquad [17]$$

Eshel and Elrod have also analyzed the effects of stiffness on the solution for the gap thickness. The following equations must be introduced for the balance of forces and moments of a foil element. These equations modify equation [5].

$$dT/ds + Q/R + \tau = 0 \qquad [18]$$

$$P - P_o = -\sigma U^2/R + T/R - dQ/ds \qquad [19]$$

$$dM/ds - Q = 0 \qquad [20]$$

$\tau = (-h/2r_o)(dP/d\theta) \pm U/h$, the fluid shear traction on the foil

$M = D/R$, the bending moment per unit width

$D = Et^3/12(1 - \gamma^2)$, the flexural rigidity of the foil per unit width

E = the modulus of elasticity

t = the foil thickness

γ = the Poisson ratio

In this developement the stiffness parameter is introduced

$$S = D\epsilon^{-2/3}/T_{\infty}r_o^2$$

This parameter relates the moment in the foil to the moment of the tension about the center of the cylinder. The same method of analysis is employed as in the derivation of [17] above. The result of this analysis is presented as a correction to equation [17] in the form of curve, Figure 2.

In Eshel's most recent analysis of the foil bearing problem (17), he includes both inertia and compressibility effects. He seeks a solution to the Navier-Stokes equations and assumes only isothermal, two-dimensional, steady flow and a perfectly flexible foil. He introduces the following non-dimensional parameters.

$C = P_o r_o/T$, the compressibility parameter, which relates atmospheric pressure to the average pressure above atmospheric under the foil

$I = \frac{1}{2}\rho U^2 r_o/T$, the inertia parameter, which relates inertia forces to the average pressure above atmospheric under the foil

The following non-dimensional variables are also employed to reduce the Navier-Stokes equations.

$$\hat{v} = U_r/U\epsilon^{-k}$$

$$\hat{u} = U_\theta/U$$

$$\eta = (y/r_o)\epsilon^{-n}$$

Now the following conditions are imposed on the problem.

(a) The expansion of equation [6] for the curvature must retain the capability of satisfying the condition that the foil becomes flat at ∞;

(b) Some inertia term must be the same order as some viscous term;

(c) Lateral and longitudinal terms in the continuity equation will be of the same order.

With these assumptions and the parameters and variables introduced above, Eshel shows that the Navier-Stokes equation reduce to the zeroth order of approximation to Prandtl's boundary layer equations.

$$I(1 + \pi/C)\,\hat{u}(\partial\hat{u}/\partial\xi) + \hat{v}(\partial\hat{u}/\partial\eta) = -\tfrac{1}{2}\partial\pi/\partial\xi + 1/12\,\partial^2\hat{u}/\partial\eta^2 \qquad [21]$$

$$\partial/\partial\eta\left\{(C + \pi)\hat{v}\right\} + \partial/\partial\xi\left\{(C + \pi)\hat{u}\right\} = 0 \qquad [22]$$

$$\pi = 1 - \partial^2 H/\partial\xi^2 \qquad [23]$$

When these equations are solved simultaneously by numerical methods, a family of curves is obtained relating H^*, I, and C. These curves are corrections for the solution for H^* in equation [17]. One of these curves is presented in Figure 3. The following equation has been fitted to those curves for the region

$$0 < 1/C < 1$$

$$0 < I < .5$$

$$H^* = .643 + .286I + 1.905I^2 - .183/C \quad . \qquad [24]$$

4. Experimental Procedure

The purpose of this experiment is to study the effect of foil stiffness on the gap thickness in an air lubricated, self-acting, foil bearing. Eshel (6) has shown that the effects of stiffness on foil gap are related by the stiffness parameter, $S = D\epsilon^{-2/3} / Tr_o^2$ which is the ratio of the moment in the foil to the moment of the foil tension about the rotor center. Then for fixed tension, the stiffness parameter increases as the foil bearing number, $\epsilon = 6\mu U/T$, decreases. The method of approach is to fix the foil tension and run an air driven, cylindrical rotor up to high speed. As the rotor is slowed, the stiffness parameter increases due to the effect of the rotor speed on the foil bearing number.

The rotor is two inches in diameter and 7.1 inches long, Figure 7. The rotor is made of stainless steel and the 4.2 inch long center section and end faces have been precision ground to a number four finish. Both waviness and roughness are critical. One inch long, pressurized air journal bearings are located at each end of the center section to support the rotor and fix its position. Pressurized air thrust bearings are located at each end face of the rotor.

A two inch wide, one one-thousandth inch thick, stainless steel foil is wrapped around the center of the rotor, passed over guides, and weighted to provide tensioning. A mechanism for changing the angle of wrap of the foil is provided. An illustration of the apparatus is provided in Figure 4.

The journal bearings are mounted in large 7-3/4 inch diameter plates. A Bently-Nevada type 318 AJX inductance probe is mounted to one of the plates and faces into the rotor halfway between the two plates. The plates ride on ball bearings which are mounted to the support base. The foil is also mounted to this base. This arrangement permits determination of the foil gap width as well as scanning of the foil contour.

The probe measures the distance to the foil. When the rotor is not turning, a reference reading is taken with the foil in contact with the rotor. Comparison of probe readings with the reference readings for any velocity gives the foil gap thickness subject to a small correction. Reference readings must be taken for each foil tension because a change in foil tension may change the position of the rotor centerline.

Additional probes are mounted at either end of the rotor. The output from these probes is displayed on two oscilloscopes, one for each end of the rotor. These displays indicate the orbit of the rotor centerline and any translation of the center from the reference position.

The rotor is driven by air turbines. These turbines are symmetrically located at either end of the rotor (see Figure 7).

Maximum shaft speed is about 800 rps with minimum foil tension of .39 lb/in. Full throttle shaft speed for a tension of 7.5 lb/in was 600 rps.

Experimental procedure is as follows:

The foil is tensioned by placing appropriate weights in the weight pan. The reading of the foil probe is recorded. The oscilloscope traces are centered. The shaft is brought up to maximum speed. After steady state is attained (constant shaft speed) the foil probe reading is recorded. The rotor orbit and the movement of the rotor center is recorded from each oscilloscope. This completes the readings for one speed. The rotor is now slowed to a new speed and the above procedure is repeated. This process is continued until constant shaft speed can no longer be maintained. When this situation occurs the data run is complete and the shaft is stopped and the reference reading re-checked. A new weight is then added to the weight pan and the above procedure is repeated.

5. Instrumentation

The instrumentation for this experiment performs three functions. They are measurement of the following: (i) foil gap thickness; (ii) rotor position; and (iii) rotor speed.

Distance measurements are made with Bently-Nevada type 318 AJX probes. These probes are driven by Bently-Nevada model 3100 N detector drivers. The power supply for the drivers is a Systems Research Corporation Power Supply model 3566.

The Bently-Nevada probe-proximitor (detector driver) arrangement provides a d-c output voltage proportional to the distance from the probe to a conducting surface. The distance-voltage relationship is linear for output voltages from 4V to 14V. For stainless steel, this gives a range of about .001 to .009 inches, and provides resolution to the nearest .000005 inches with a sufficiently accurate voltage sensing device. For details on probe calibration, see Appendix A.

The output of the foil gap probe was displayed on a Hewlett Packard model 2010C digital voltmeter capable of measuring to the nearest .001 volts at 99 volts full scale. This voltmeter integrates voltage over time periods of .01, .1 and 1 second. The .1 second time period was employed.

Rotor position was determined by four other probes mounted 90° apart, two at each end of the rotor. The output from these probes was displayed on two Hewlett Packard model 130 oscilloscopes. The probe outputs were biased with 7.5 volt d-c batteries so that a zero reading could be attained

near the center of the probe linear range.

Shaft speed measurement was accomplished using a Hewlett Packard 506A optical tachometer pickup driving a Hewlett Packard model 522 electronic counter. This system is capable of measuring from 5 rps to 5,000 rps. The pickup was accomplished by blackening a 3.4 inch wide half-section of the shaft adjacent to the turbine buckets at one end.

6. Results

The results of the experimental work are presented in tabular form in Tables 1, 2, 3 and 4 and in graphical form in Figures 10, 11, 12, and 13. Figure 10 is a plot of the gap thickness h against the peripheral velocity U where the foil tension T has been held fixed for each run. Figure 11 is a plot of h against the foil bearing number, $\epsilon = \frac{6\mu U}{T}$, to the 2/3 power. This is done because in all of the theoretical works of Eshel the non-dimensional gap width is assumed to be a power series in this parameter.

Figure 12 is a plot of the nominal non-dimensional gap thickness H^* against the stiffness parameter S. Figure 13 is a plot of H^* against the inertia parameter I. This curve was constructed because the inertia parameter varies significantly throughout the range of data, and it would be useful to separate the effects of inertia from those of stiffness.

The angle of wrap of the foil for both data runs was 60 degrees. Foil tension was .39 lb/in and 1.19 lb/in for the respective data runs. Shaft speed ranged from 500 rps to 100 rps.

7. Discussion of Results

The results of this experiment are incomplete and therefore inconclusive. Only two data runs were completed due to failure of the rotor support system.

During the first attempt at a data run, the foil partially slipped out of the foil bracket. As a result, the effective width of the foil went from two inches to less than $\frac{1}{4}$ inch. This destroyed the air film between foil and rotor and in turn caused one of the bearings to fail. Due to the large dissipation of energy in such a short time, the bearing seized badly. It could not be pressed off and had to be cut off on the lathe.

The rotor was re-ground and a new bearing was manufactured. The bearing could not be ground as the proper facilities were not available. The bearing was finished by using a fine grade of emery paper. This refinished rotor and bearing were assembled and the rotor was found to be out-of-round.

The best alternative at this point seemed to be to make a new rotor and to have the existing bearings re-ground. Re-grinding the rotor was deemed impractical because it necessitated centerless grinding. No centerless grinding facilities were available.

The data was obtained using this second rotor. Preliminary testing of this rotor and support system indicated considerable imbalance but with a very low resonance point. As time was very short it was decided to press on and obtain some data.

The first two runs of data were made without difficulty. A third run of data was attempted but a higher rotor speed was necessary. This is true because as the tension is increased, the maximum speed must also be increased to maintain the same range of foil bearing number, $\epsilon = 6\mu U/T$. Each succeeding run used a higher foil tension than the one before.

On the third run synchronous whirl became evident at about 650 rps. Although the whirl orbit was increasing in size as the speed increased it was nevertheless small compared to the clearance in the bearing. At about 840 rps both journal bearings failed suddenly. It appears that a resonance occurred at or near this speed. The rotor was being accelerated slowly and although the whirl orbit was still growing slowly at about 800 rps, it seemed to be stabalizing.

Both runs of data that were obtained were runs made with constant values of foil tension. The inverse compressibility parameter, $1/C = T/P_o r_o$, is constant for both these cases. Therefore it is reasonable to neglect the compressibility effect as it pertains to one set of data.

A wide range of stiffness parameters is spanned by both runs of data, see Tables 2 and 4. Unfortunately a wide range of inertia parameters is also spanned. Recall that for fixed foil tension, the inertia parameter varies as velocity to the second power. For this reason, it is impossible to separate the two effects.

The value of $H^* = .643$ is well accepted in the foil bearing literature. The effect of inertia is to increase

this value, while compressibility and stiffness tend to decrease this value. Both runs of data indicate that the effect of stiffness for this range of speed and tension is large compared to the effect of inertia.

Comparison between the two runs indicates the effect of compressibility over a wide range of stiffness. This indication is that the effect of compressibility is significant only for small values of stiffness.

These results are more useful in determining the proper conditions for further research than they are in giving quantitative inference into the behavior of a foil bearing. They show the reader that in order to study the effects of compressibility or inertia, the stiffness effect must be minimized.

8. Recommendations for Further Work

Due to the fact that so little data was obtained, there seems to be considerable room for further work with this apparatus. Several changes need to be made before the device will work reliably and before more useful data can be obtained.

The significant stiffness effects have already been mentioned. A good project would be to eliminate these effects and attempt to isolate the effects of inertia or compressibility. A more flexible foil such as Mylar, coated with a thin conducting film, could be tried for this purpose.

Also mentioned previously, the rotor support system, specifically the journal bearings, gave considerable trouble. The bearings were made out of stainless steel, the same material as the rotor. This was done to minimize temperature effects. Consequently, when the bearings failed, considerable damage was done to both bearings and journals.

A necessary improvement would then be the re-design of the bearings so as to provide protection for the rotor in the event of failure. To this end, a material must be found that is soft compared to stainless steel, yet can be machined to the smoothness required of an air bearing. One possibility might be to re-machine the existing bearings and coat the bearing surface with a thin film of Teflon. Another possibility might be to use nylon bearings.

The cause of the last bearing failure was probably imbalance of the rotor. It is therefore recommended that

the rotor be precision balanced. The rotor run-out should be held to less than .0001 inches at speeds up to 60,000 rpm.

BIBLIOGRAPHY

1. H. Blok and J. J. van Rossum, "The Foil Bearing-A New Departure in Hydrodynamic Lubrication," Lubrication Engineering, Vol. 9, No. 6, December 1953, pp. 310 - 320.
2. B. J. Patel, "The Foil Bearing," Conference on Lubrication and Wear, The Institute of Mechanical Engineers, London, October 1957, Paper No. 73.
3. H. K. Baumeister, "Nominal Clearance of the Foil Bearing," IBM Journal, Vol. 7, No. 2, April 1963, pp. 153 - 154.
4. H. K. Baumeister, "Further Considerations on the Nominal Clearance of the Foil Bearing," ASLE Annual Meeting, Chicago, 1964, Paper No. 5B5.
5. A. Eshel and H. G. Elrod, "The Theory of the Infinitely Wide, Perfectly Flexible Foil Bearing," ASME, Paper No. 65-Lubs-3.
6. A. Eshel and H. G. Elrod, "Stiffness Effects on the Infinitely Wide Foil Bearing," ASME, Paper No. 66-Lubs.-6.
7. A. Eshel and H. G. Elrod, "Compressibility Effects on the Infinitely Wide, Perfectly Flexible Foil Bearing," ASME, Paper No. 67-Lub-2.
8. L. Licht, "Preliminary Experiments With Foil Bearings," Journal of Basic Engineering, Trans. ASME, Series D, Vol. 88, No. 1, March 1966, pp. 1-3.

9. L. Licht, "An Experimental Study of Air-lubricated Foils With Reference to Tape Transport in Magnetic Recording," Report No. 7, Columbia University, New York, prepared under Contract Nonr-4259(14) Task NR 062-360, Information Systems Branch and Fluid Dynamics Branch, ONR.

10. L. Licht, "An Experimental Study of Elastohydrodynamic Lubrication of Foil Bearings," ASME, Paper No. 67-Lub-3.

11. J.T. S. Ma, "An Investigation of Self-Acting Foil Bearings," Journal of Basic Engineering, Trans. ASME, Series D, Vol. 87, No. 4, December 1965, pp. 837- 846.

12. W. A. Gross, Gas Film Lubrication, John Wiley & Sons, New York, New York.

13. N. S. Grassam and J. W. Powell, Gas Lubricated Bearings, Butterworth and Company LTD, London, England.

14. M. Wildmann, "Foil Bearings - Their General Behavior With Particular Emphasis on the Externally Pressurized Bearing," Ampex Report RR64-13, December 1964.

15. A. F. Stahler and A. Huckabay, "Analyzation, Design, Fabrication, and Testing of a Foil Bearing Rotor Support System," Ampex Report RR66-21, June 1966.

16. L. Licht and A. Eshel, "Study, Fabrication and Testing of a Foil Bearing Rotor Support System," Ampex Report RR68-2, April 1968.

17. A. Eshel, "On Fluid Inertia Effects In Infinitely Wide Foil Bearings," Ampex Report RR68-15, July 1968.

TABLE 1.

Measured Quantities, 1st Run

Foil Tension lb/in	Shaft Speed rps	Gap Thickness volts
.39	452	.735
	428	.700
	416	.670
	393	.625
	360	.550
	300	.428
	250	.319
	199	.230
	152	.140
	101	.058

TABLE 2

Computed Quantities, 1st Run

Gap Thickness inches	Foil Bearing Number X 10^6	Inertia Parameter	Stiffness Parameter	Inverse Compressibility Parameter
.000735	118	1.1	2.93	.026
.000700	112	.98	3.04	
.000670	109	.93	3.08	
.000625	103	.82	3.20	
.000550	95	.69	3.41	
.000428	78	.48	3.81	
.000319	66	.34	4.33	
.000230	52	.21	5.06	
.000140	39	.12	6.06	
.000058	26	.05	7.80	

TABLE 3.

Measured Quantities, 2nd Run

Foil Tension lb/in	Shaft Speed rps	Gap Thickness volts
1.19	775*	.730*
	492	.361
	451	.333
	404	.282
	350	.254
	300	.220
	242	.177
	189	.150
	160	.133

* These measurements made at an earlier time than the rest.

TABLE 4.

Computed Quantities, 2nd Run

Gap Thickness inches	Foil Bearing Number X 10^6	Inertia Parameter	Stiffness Parameter	Inverse Compressibility Parameter
.000730*	67*	1.04*	1.40*	.08
.000361	42	.42	1.88	
.000333	39	.36	2.00	
.000282	35	.28	2.16	
.000254	30	.21	2.39	
.000220	26	.16	2.68	
.000177	21	.10	3.03	
.000150	15	.07	3.78	
.000133	14	.05	4.01	

* These measurements made at an earlier time than the rest.

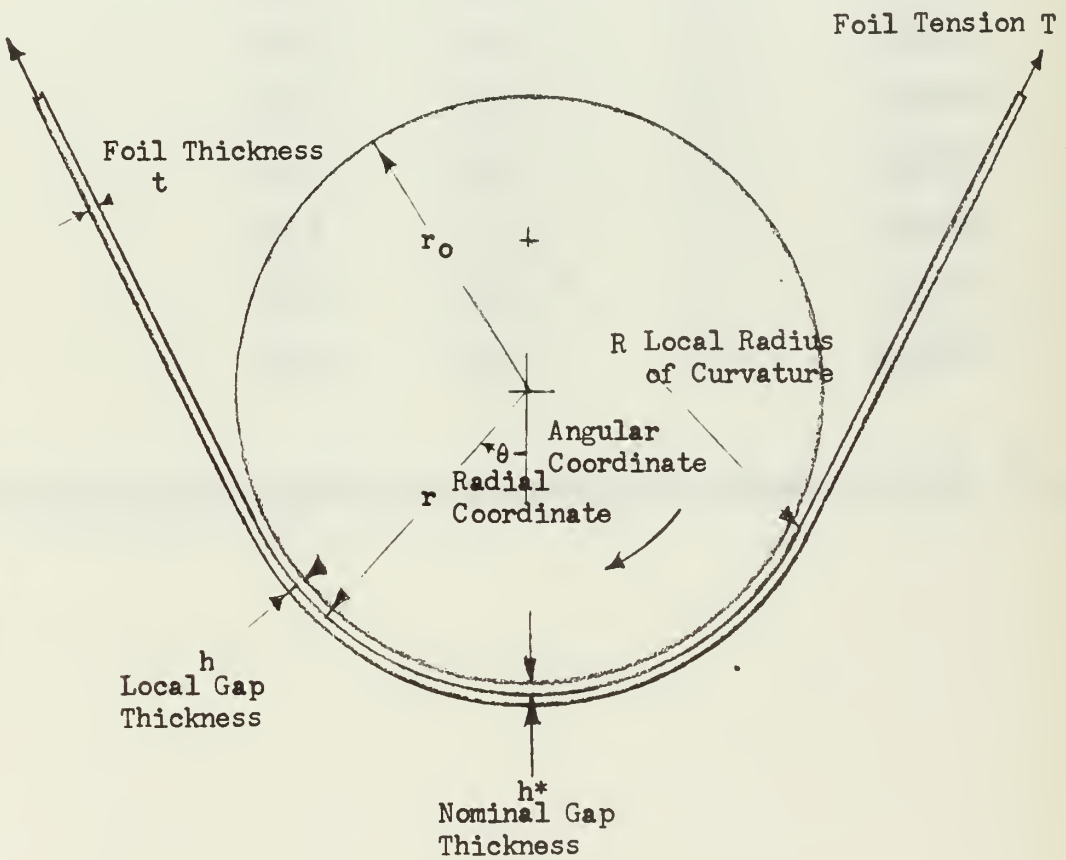


FIGURE 1. SCHEMATIC OF FOIL TYPE BEARING

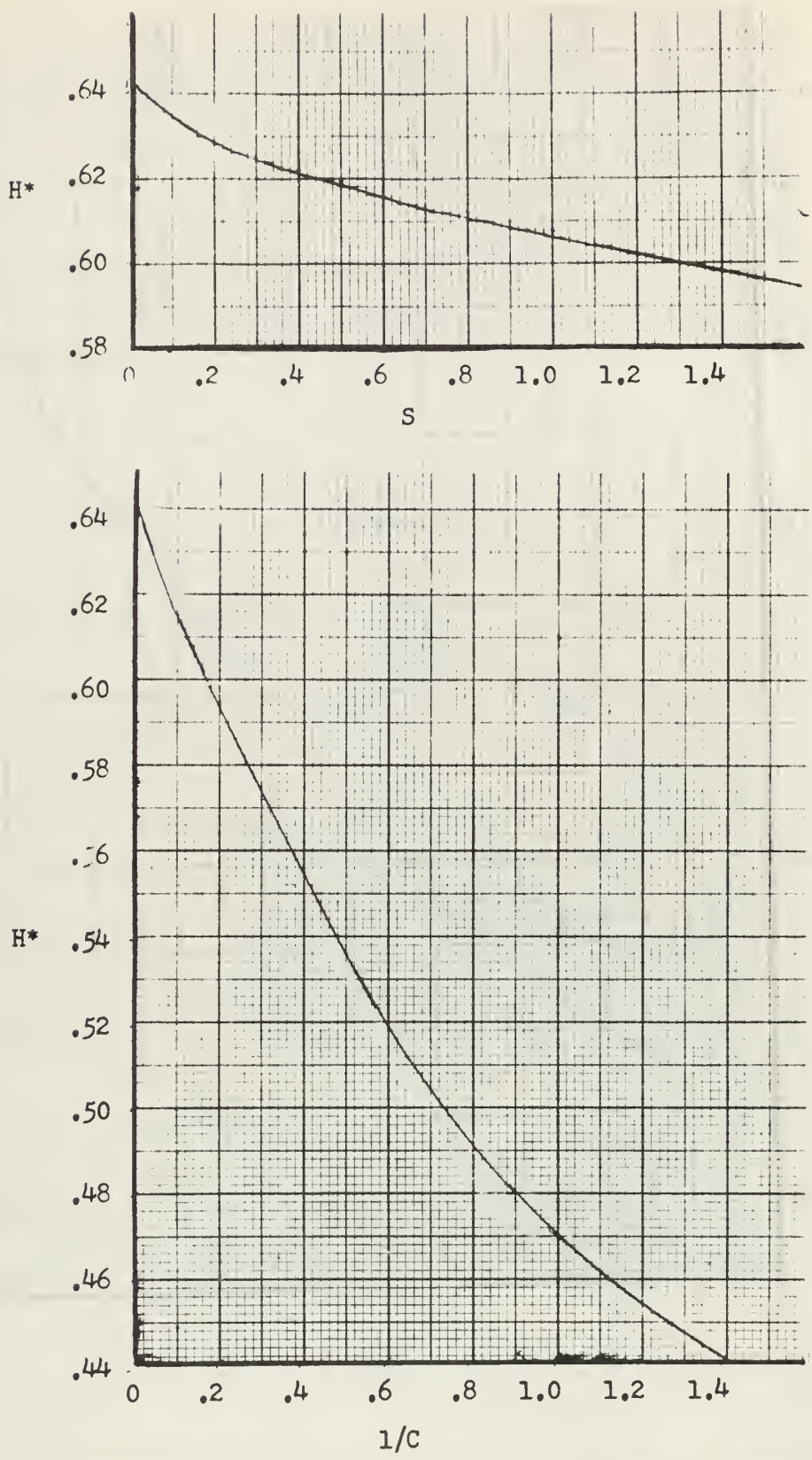


FIGURE 2. NOMINAL CLEARANCE VERSUS STIFFNESS AND COMPRESSIBILITY PARAMETERS

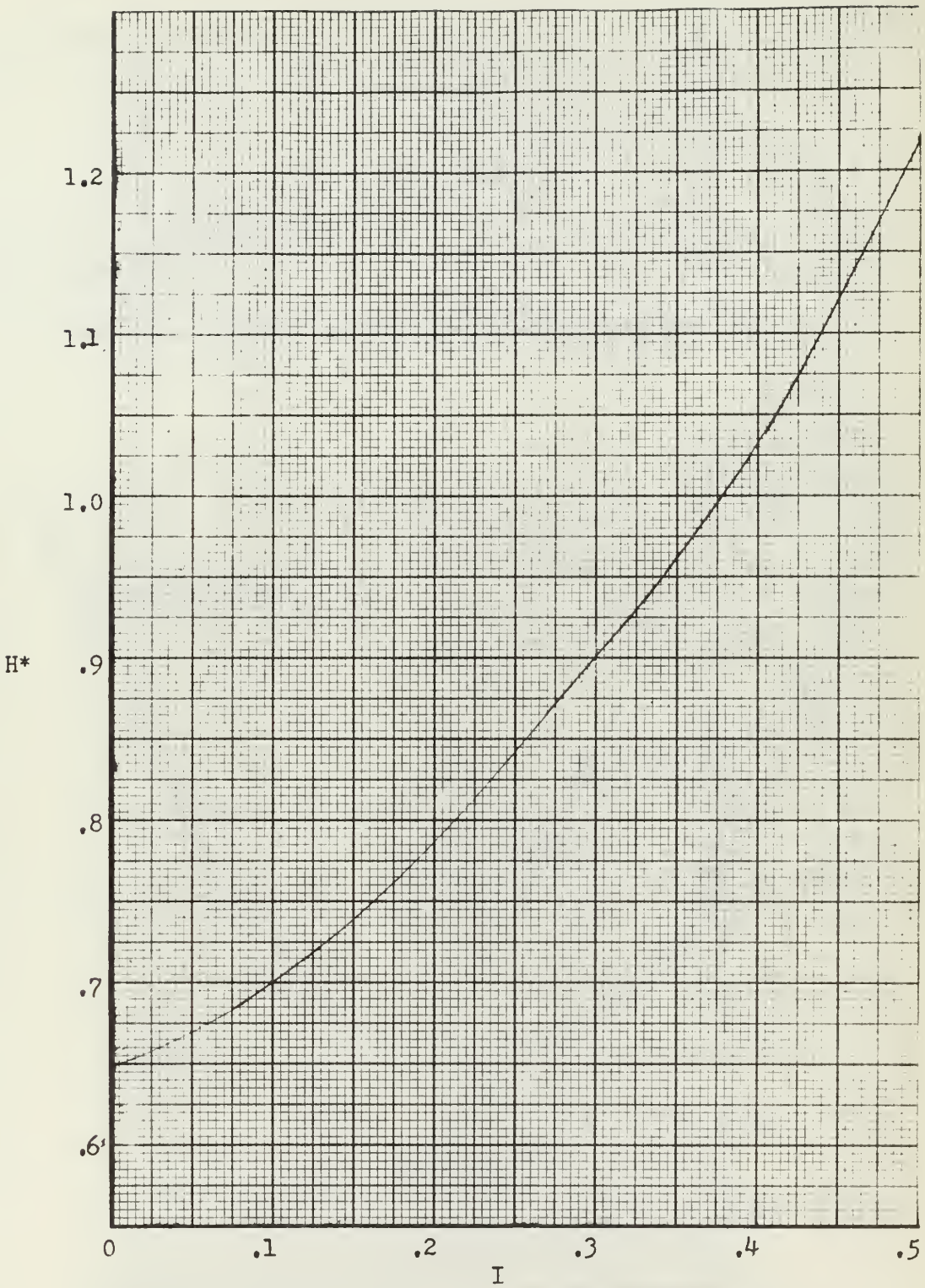


FIGURE 3. NOMINAL CLEARANCE VERSUS INERTIA PARAMETER
(from Eshel (17))

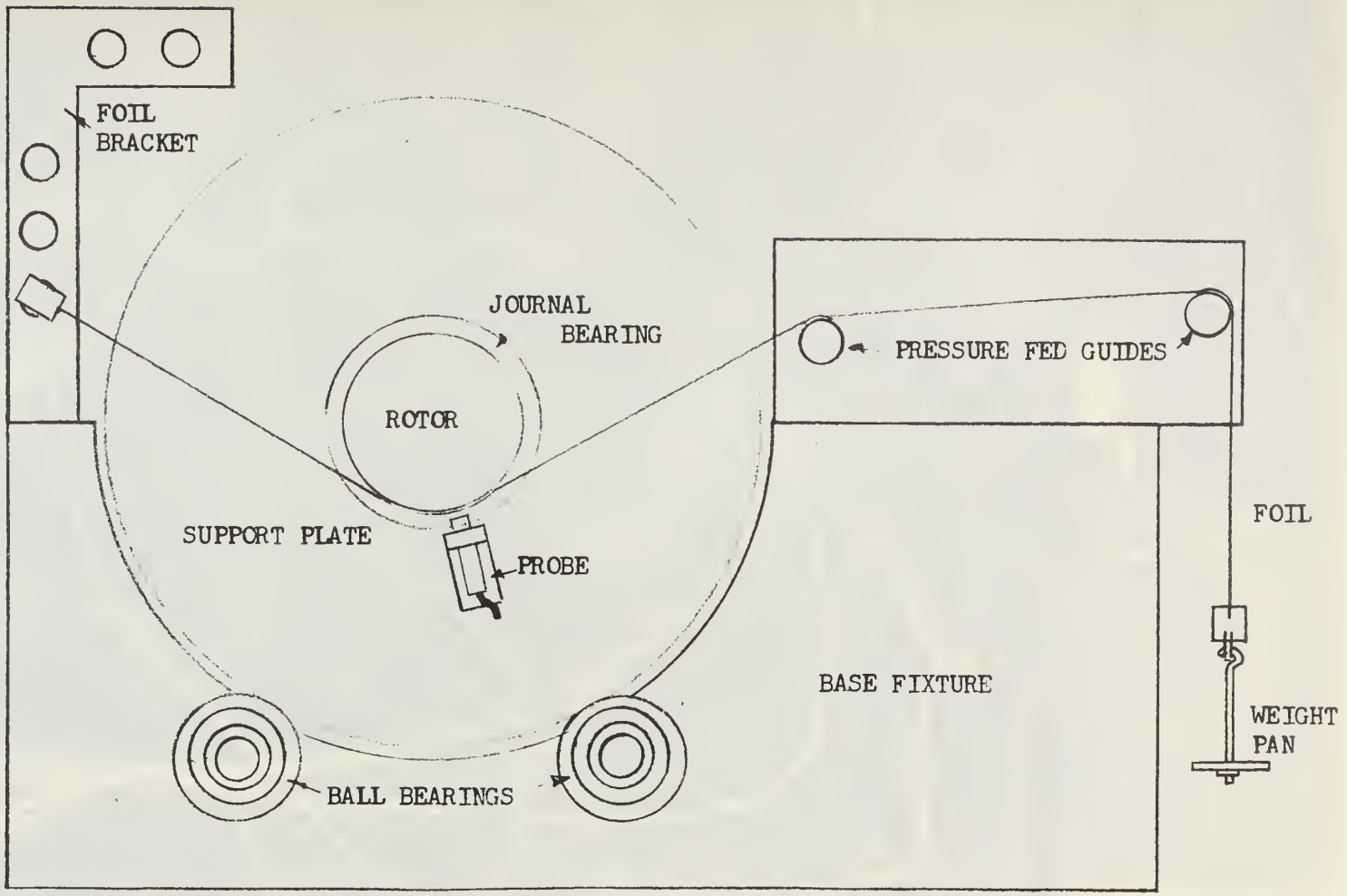


FIGURE 4. CUT-AWAY VIEW OF TEST APPARATUS

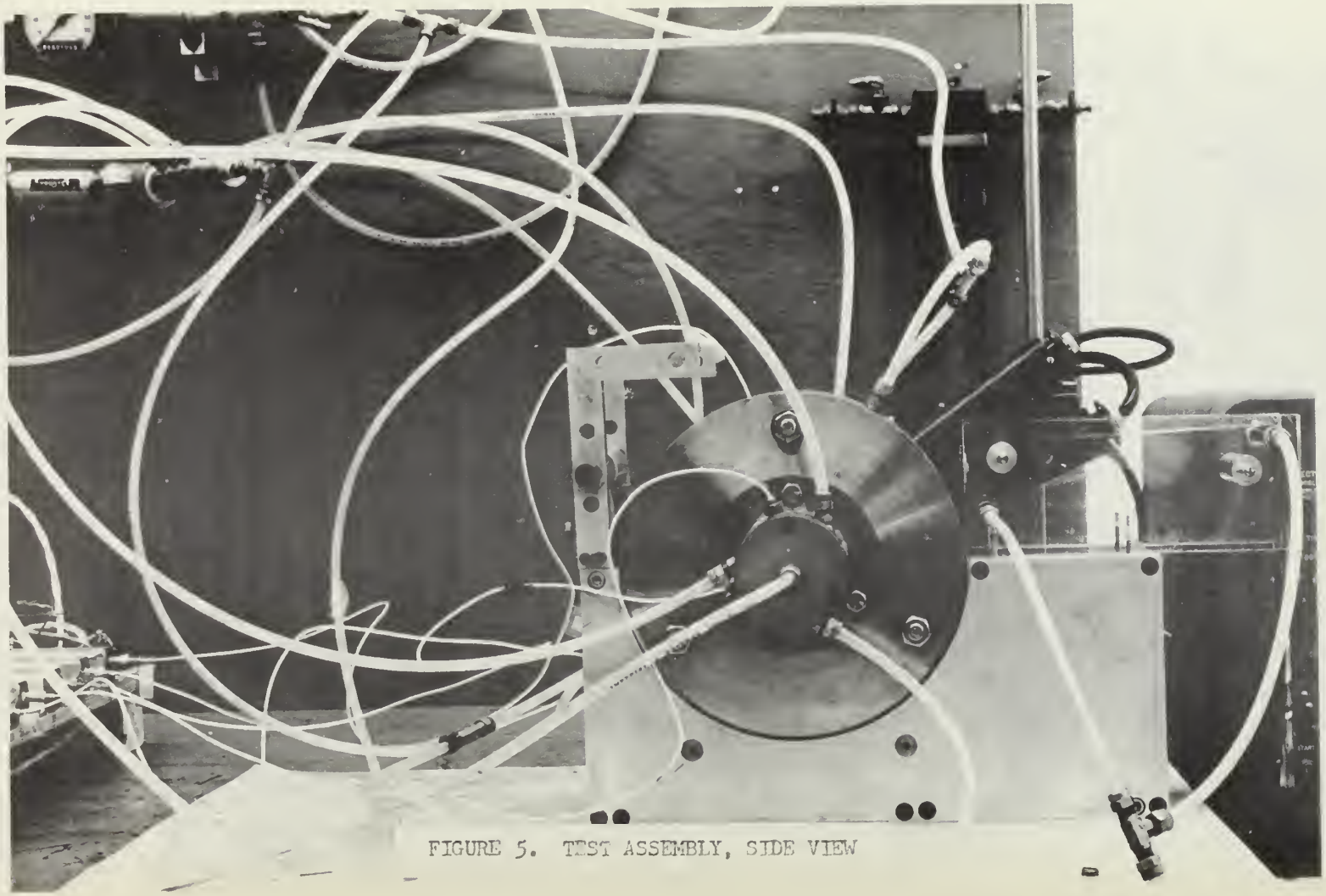


FIGURE 5. TEST ASSEMBLY, SIDE VIEW

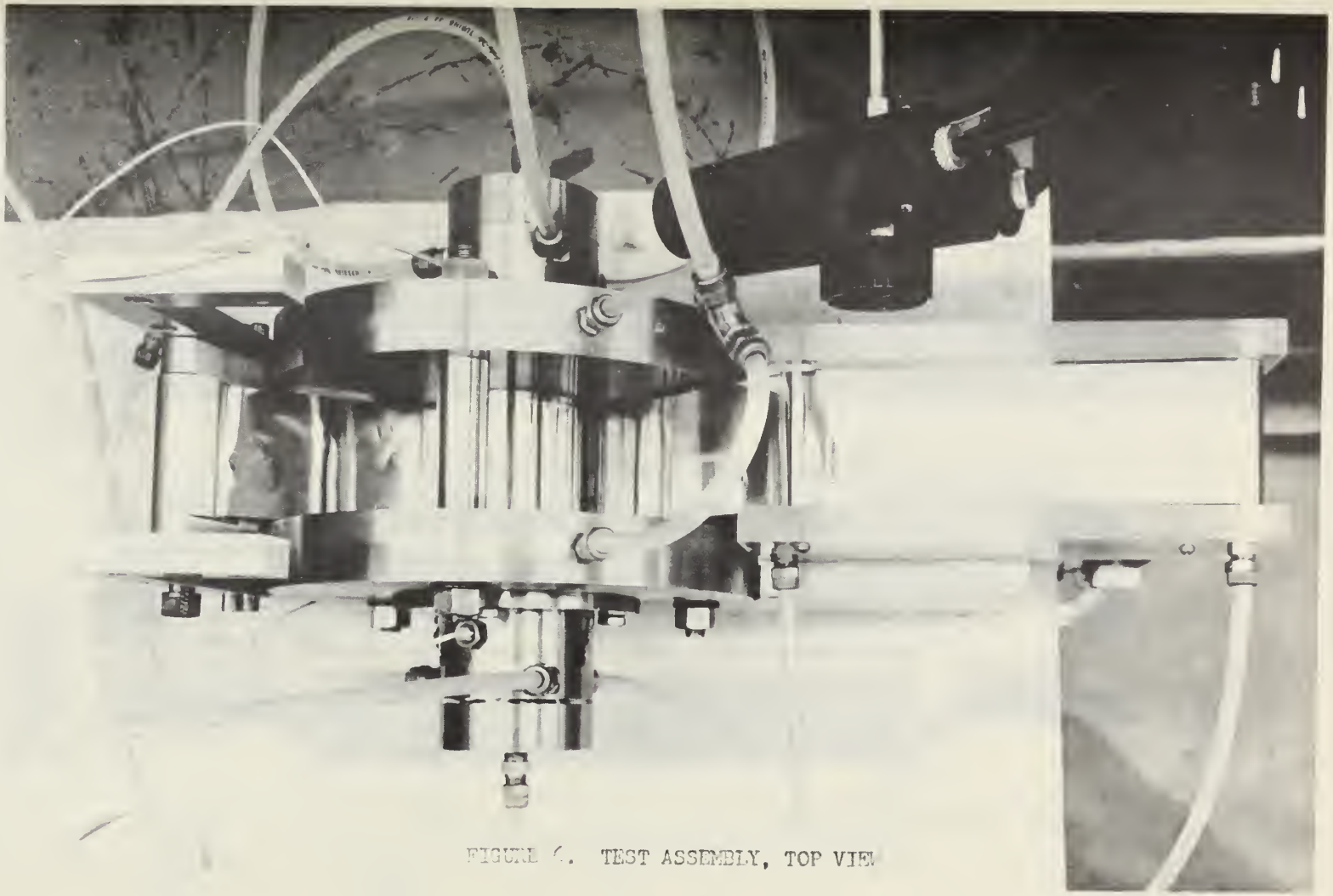


FIGURE 4. TEST ASSEMBLY, TOP VIEW

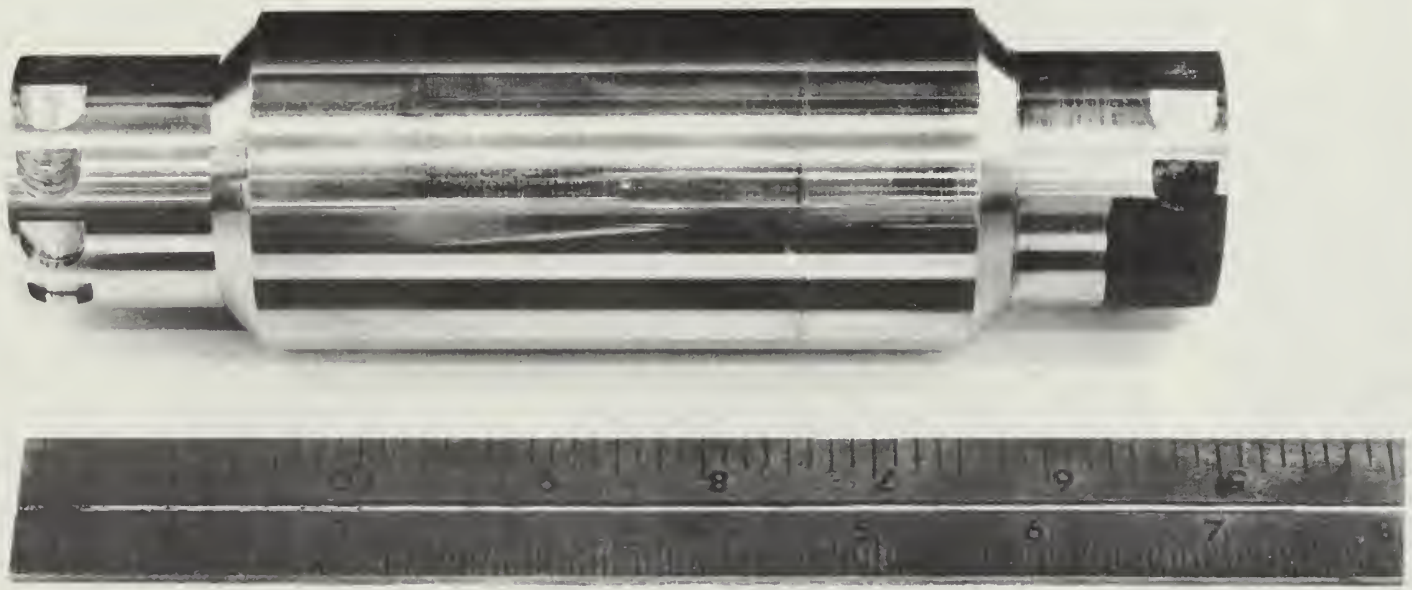


FIGURE 7. ROTOR

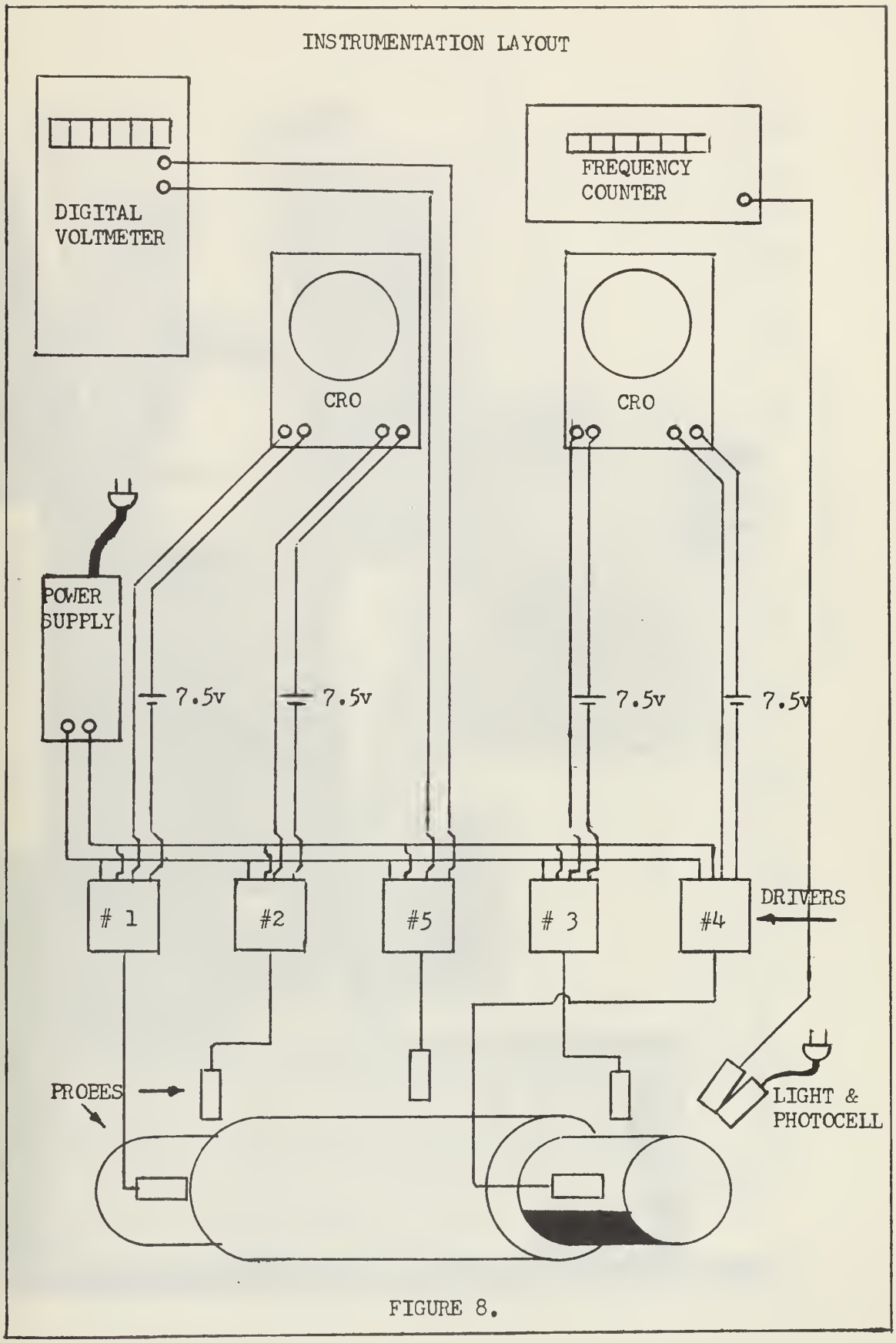

INSTRUMENTATION LAYOUT
DIGITAL VOLTMETER
FREQUENCY COUNTER
CRO
CRO
POWER SUPPLY
7.5v
7.5v
7.5v
7.5v
1
#2
#5
3
#4
DRIVERS
PROBES
LIGHT & PHOTOCELL

FIGURE 8.

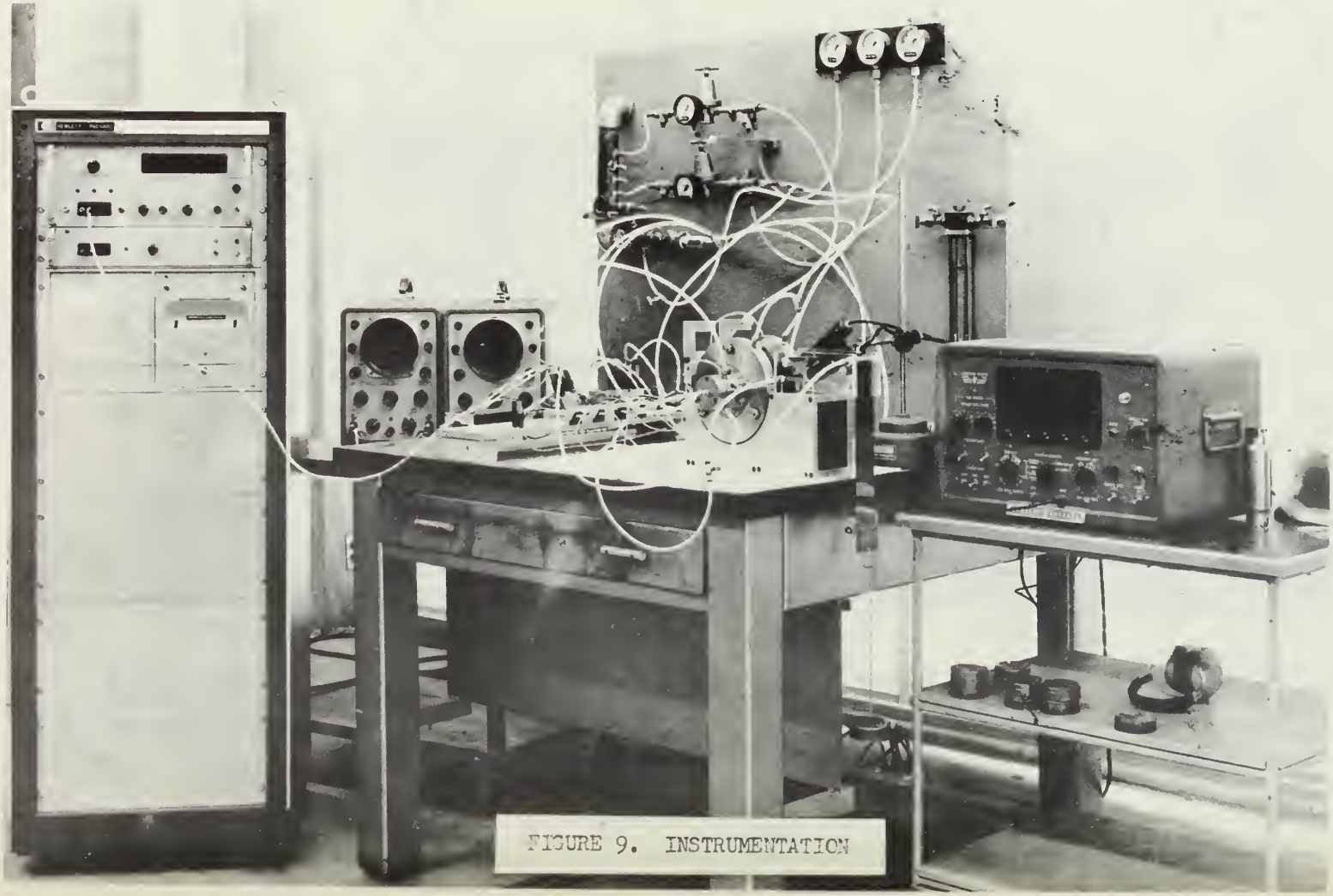


FIGURE 9. INSTRUMENTATION

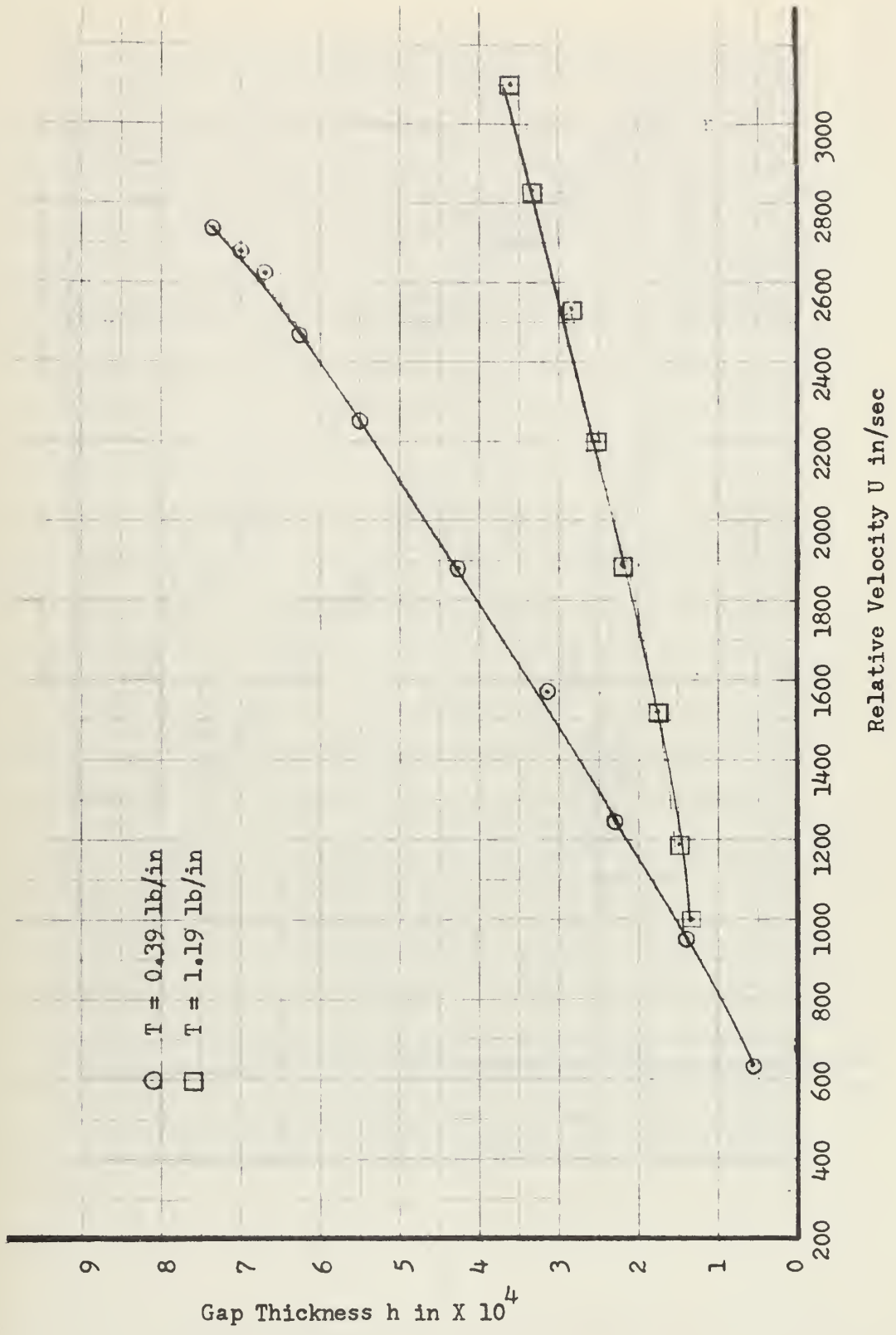


FIGURE 10. GAP THICKNESS VERSUS RELATIVE VELOCITY

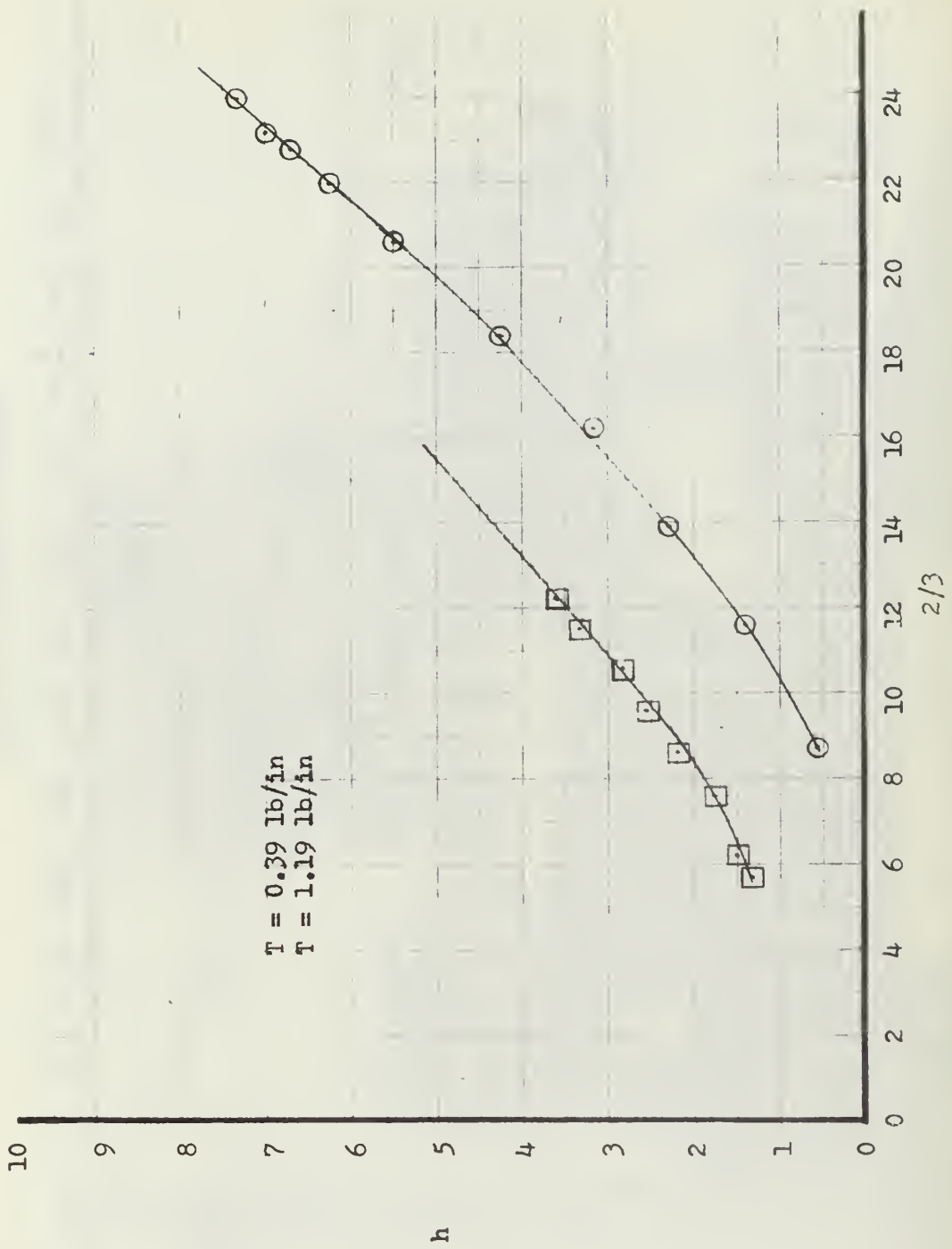


FIGURE 11. GAP THICKNESS VERSUS FOIL BEARING NUMBER

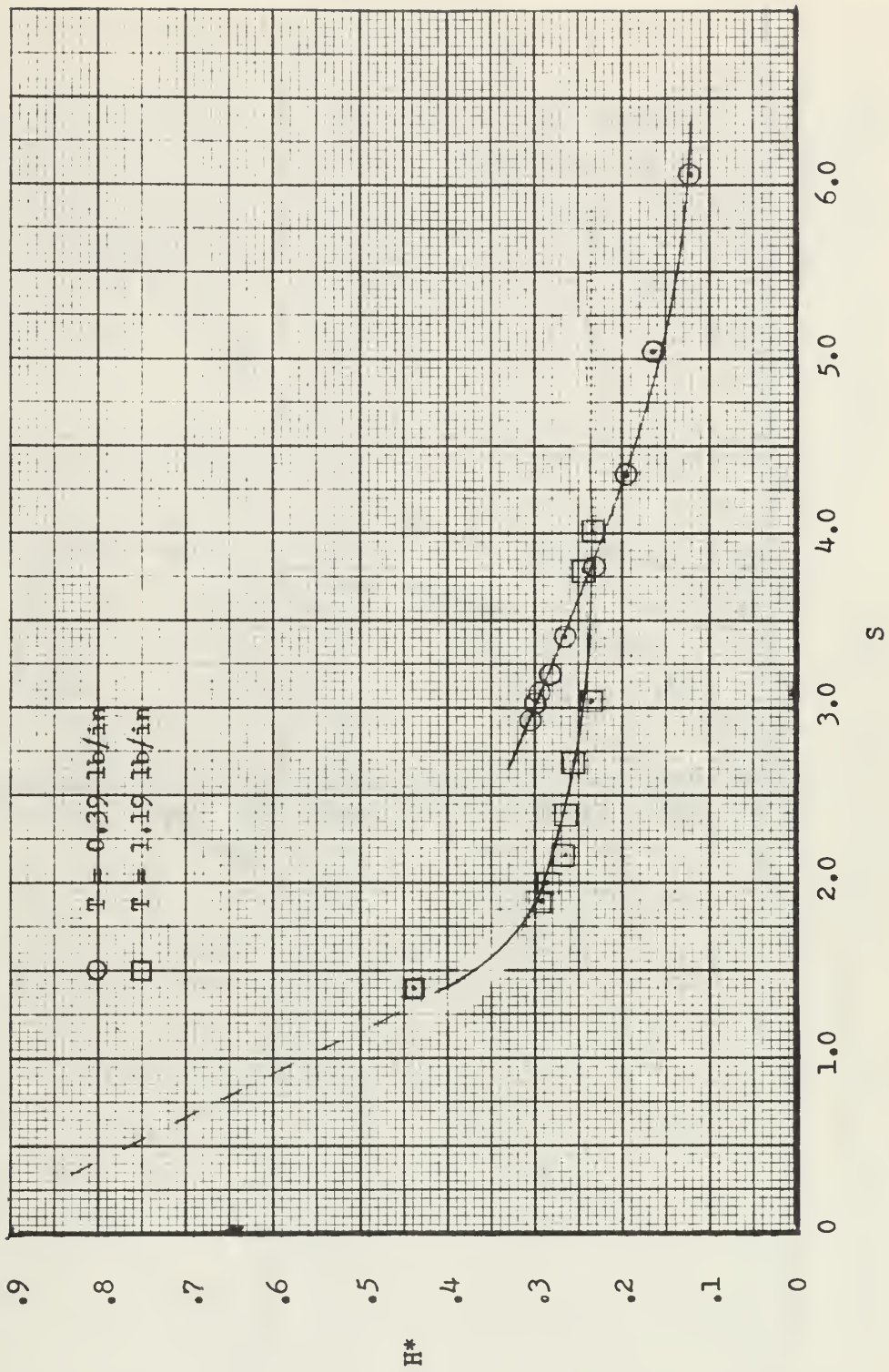


FIGURE 12. NOMINAL CLEARANCE VERSUS STIFFNESS PARAMETER

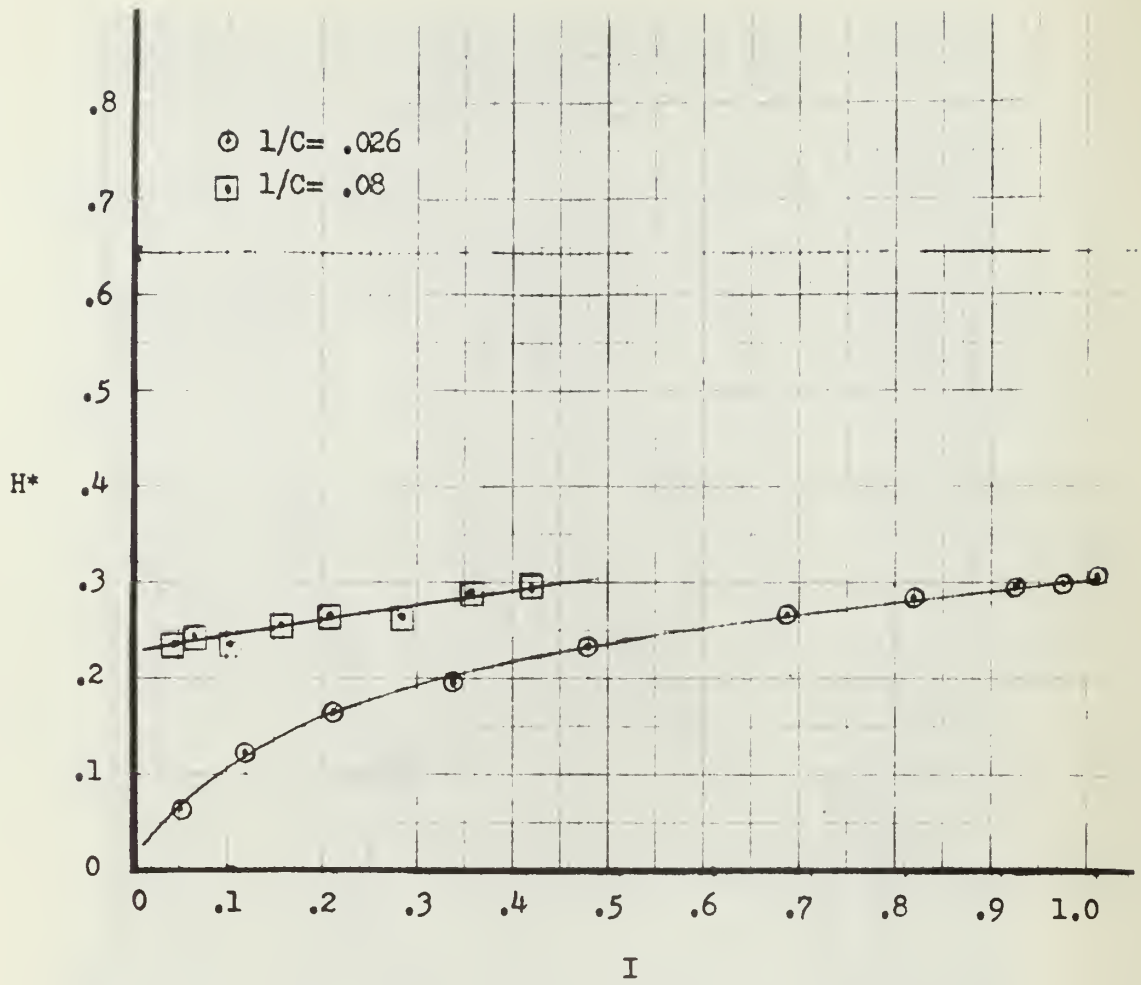


FIGURE 13. NOMINAL CLEARANCE VERSUS INERTIA PARAMETER

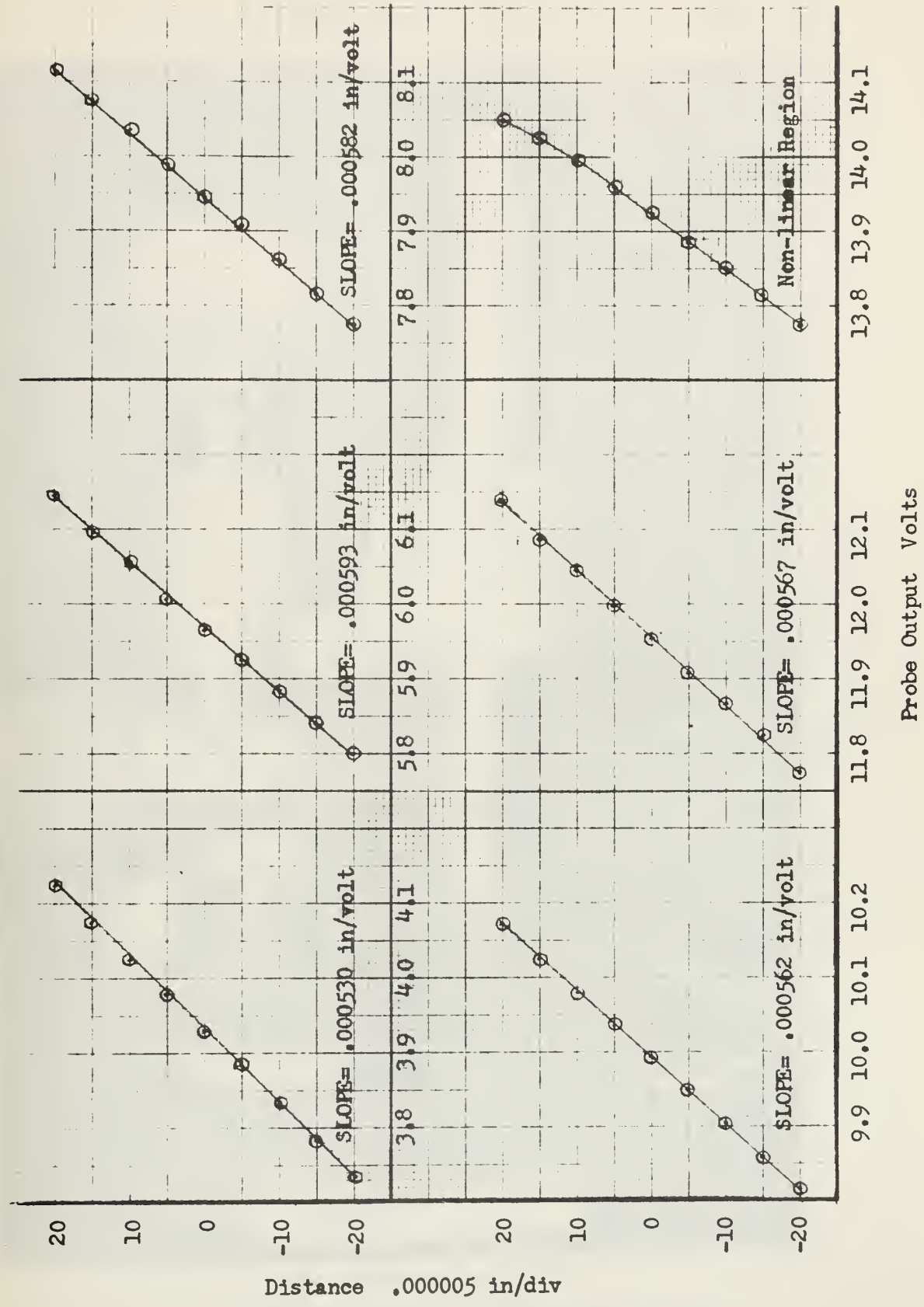


FIGURE 14. DISTANCE PROBE CALIBRATION CURVES

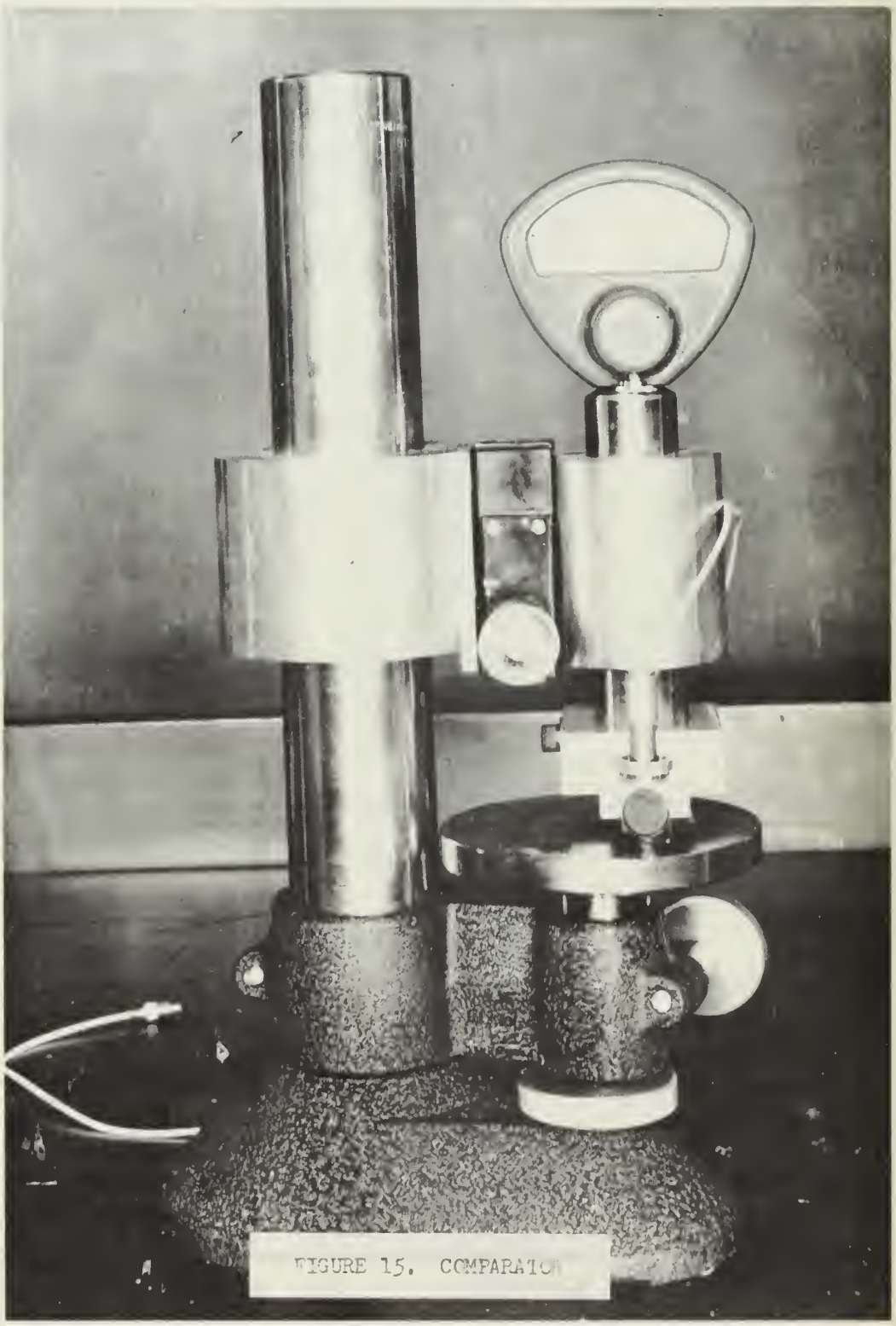


FIGURE 15. COMPARATOR

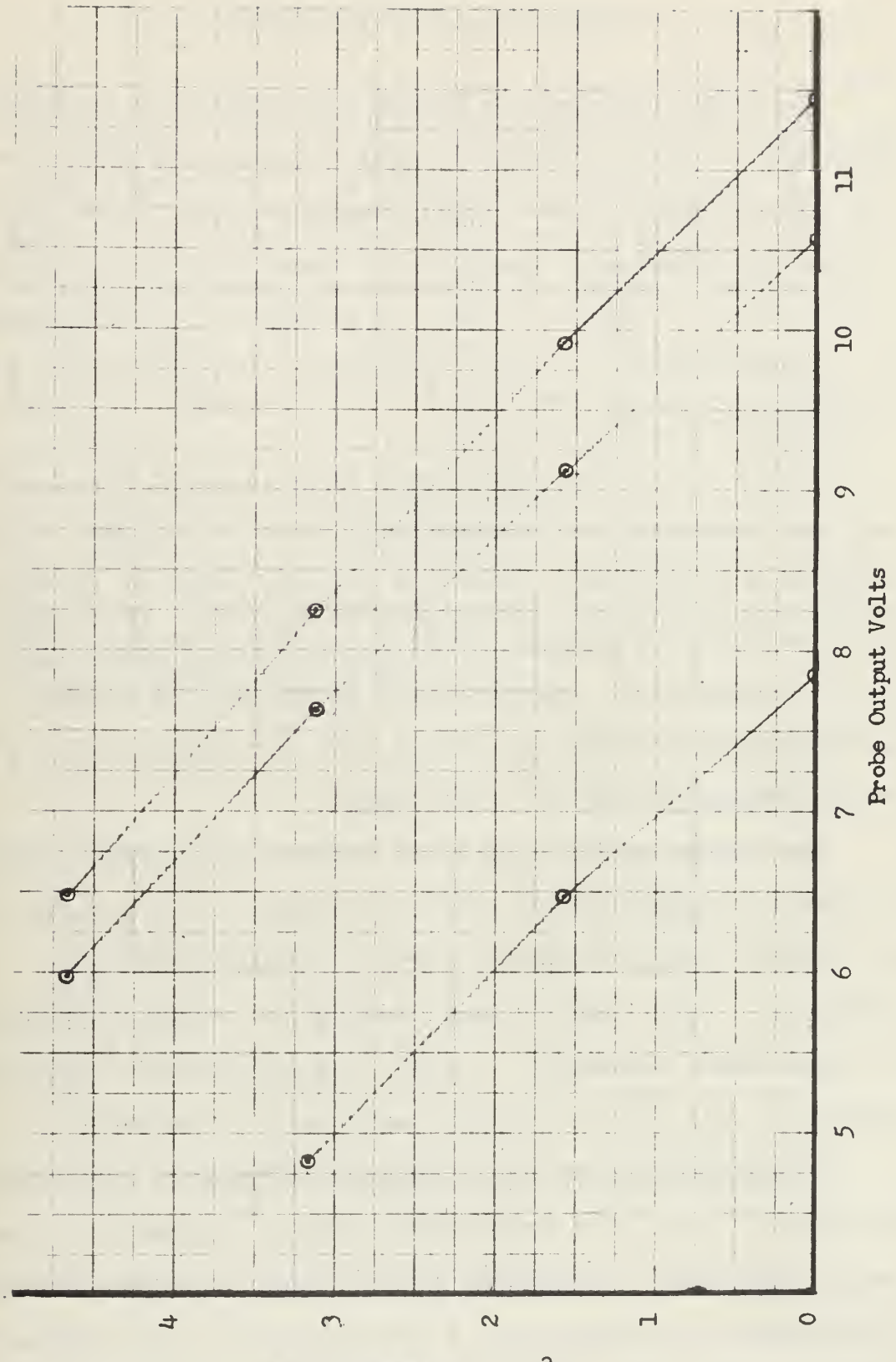


FIGURE 16. FOIL GAP CALIBRATION CURVE

PROBE CALIBRATION APPENDIX

The probe calibration system consisted of a Johannson Mikrokator model S510E-7 comparator which is accurate to the nearest .000005 inch. The comparator was fitted with a micrometer adjustment mechanism salvaged from a microscope. A fixture for holding a probe was attached to this mechanism. The calibration disc in the comparator was made of the same material as the rotor.

Moving the probe up and down with the micrometer adjustment and recording the voltage output on the digital voltmeter provided a calibration curve for a small range of voltage. This was done for several nominal voltages for each probe-driver combination. These curves establish the linear operating range of the probe and give the slope of the voltage versus distance line for that range.

The probes were checked for temperature effects and the following conclusions have been reached: (i) The slope of the voltage versus distance curve is not temperature sensitive. (ii) The voltage reading for a given distance is temperature sensitive. (iii) The drivers are temperature sensitive, but only for large variations of temperature.

These effects are not considered to effect significantly the results since the probes are located in positions where large temperature variations do not occur. Driver (ambient) temperature is constant for a given data run, and varies only slightly (less than 10°) over all runs. A calibration curve has been provided in Figure 14.

Calibration for the foil gap measurement was accomplished in the following manner. Several thin paper shims were measured for thickness with one of the probes mounted in the comparator. The shims were then inserted between the foil and the rotor. The reading on the digital voltmeter was then recorded. A shim was then removed and another reading taken. This procedure was continued until the gap measuring probe was out of its linear range of operation. The foils were then inserted again in turn and readings were taken until the original number were in place. From this data a curve was obtained for gap thickness versus probe output voltage differential. The resulting calibration curve is presented as Figure 16.

INITIAL DISTRIBUTION LIST

		Copies
1.	Defense Documentation Center Cameron Station Alexandria, Virginia	20
2.	Library Naval Postgraduate School Monterey, California	2
3.	Naval Ship System Command Navy Department Washington, D.C. 20360	1
4.	Professor Paul Pucci Department of Mechanical Engineering Naval Postgraduate School Monterey, California	1
5.	Department of Mechanical Engineering Naval Postgraduate School Monterey, California	1
6.	Lt. John M. Knight Board of Inspection and Survey Sub-board San Diego Naval Station San Diego, California	3
7.	Dr. Abe Eshel Ampex Corporation (MS 3-20) 401 Broadway Redwood City, California	1
8.	LCDR Sompong Phasook RTN 90 Soi Baring (Banga) Bangkok, Thailand	1
9.	Mr. John W. Knight, Jr. Land Department Pacific Gas and Electric Co. 245 Market Street San Francisco, California	1

DOCUMENT CONTROL DATA - R & D

(Security classification of title, body of abstract and indexing annotation must be entered when the overall report is classified)

1. ORIGINATING ACTIVITY *(Corporate author)*
Naval Postgraduate School
Monterey, California 93940

2a. REPORT SECURITY CLASSIFICATION
UNCLASSIFIED

2b. GROUP

3. REPORT TITLE
AN EXPERIMENTAL STUDY OF A SELF-ACTING FOIL BEARING AT LOW VALUES OF FOIL TENSION

4. DESCRIPTIVE NOTES *(Type of report and inclusive dates)*
Thesis

5. AUTHOR(S) *(First name, middle initial, last name)*
John Michael Knight, Lieutenant, United States Navy

6. REPORT DATE
September 1968

7a. TOTAL NO. OF PAGES
59

7b. NO. OF REFS
17

8a. CONTRACT OR GRANT NO.

b. PROJECT NO.

c.

d.

9a. ORIGINATOR'S REPORT NUMBER(S)

9b. OTHER REPORT NO(S) *(Any other numbers that may be assigned this report)*

10. DISTRIBUTION STATEMENT
[redacted]

11. SUPPLEMENTARY NOTES

12. SPONSORING MILITARY ACTIVITY
Naval Postgraduate School
Monterey, California 93940

13. ABSTRACT

Theoretical solutions for the gap thickness in an infinitely wide foil bearing are reviewed. An experiment is described using a stainless steel foil wrapped about a high speed rotor. Details of instrumentation are included. Results are presented for the relation between gap thickness and foil stiffness for low values of foil tension.

Only a small amount of data was obtained due to failure of the rotor support mechanism . The results are therefore inconclusive. The results do, however, indicate a dependence of foil gap thickness on foil stiffness. The influence of fluid inertia on foil gap thickness is also indicated although this effect appears to be small compared to the effects of foil stiffness.

14 KEY WORDS	LINK A		LINK B		LINK C	
	ROLE	WT	ROLE	WT	ROLE	WT
Foil Bearings						
Fluid Mechanics						
Fluid Films						
Stiffness Effects						
Gas Lubrication						



thesK62
DUDLEY KNOX LIBRARY
3 2768 00416530 8
DUDLEY KNOX LIBRARY